Neurochem Res (2007) 32:1142–1149
DOI 10.1007/s11064-007-9282-4

ORIGINAL PAPER

Effect of Hyperoxia on Cortical Neuronal Nuclear Function and Programmed Cell Death Mechanisms

Eddie Chang · Kristie Hornick · Karen I. Fritz · Om P. Mishra · Maria Delivoria-Papadopoulos

Accepted: 4 January 2007 / Published online: 31 March 2007

Abstract There is growing concern over detrimental neurologic effects to human newborns caused by increased inspired oxygen concentrations. We hypothesize that hyperoxia ($FiO_2 > 0.95$) results in increased high-affinity Ca^{2+}-ATPase activity, Ca^{2+}-influx, and proapoptotic protein expression in cortical neuronal nuclei of newborn piglets. Neuronal cerebral energy metabolism was documented by determining ATP and phosphocreatine levels. Neuronal nuclear conjugated dienes and fluorescent compounds were measured as indices of lipid peroxidation. High-affinity Ca^{2+}-ATPase activity and ATP-dependent Ca^{2+}-influx were determined to document neuronal nuclear membrane function. Hyperoxia resulted in increases in lipid peroxidation, high-affinity Ca^{2+}-ATPase activity, ATP-dependent Ca^{2+}-influx, and Bax/Bcl-2 ratio in the cortical neuronal nuclei of newborn piglets. We conclude that hyperoxia results in modification of neuronal nuclear membrane function leading to increased nuclear Ca^{2+}-influx, and propose that hyperoxia-induced increases in intranuclear Ca^{2+} activates the Ca^{2+}/calmodulin-dependent protein kinase pathway, triggering increased CREB protein-mediated apoptotic protein expression in hyperoxic neurons.

Keywords Apoptosis · ATP · Bax · Bcl-2 · Hyperoxia · High affinity Ca^{2+}-ATPase · Intranuclear Ca^{2+}-influx · Lipid peroxidation · Mechanism · Neuron · Nuclear function · Newborn piglet · Oxidative stress · Phosphocreatine

E. Chang (✉) · K. Hornick · K. I. Fritz · O. P. Mishra · M. Delivoria-Papadopoulos
Department of Pediatrics, St. Christopher's Neonatal Research, Drexel University College of Medicine, 245 N. 15th Street, Mail Stop 1029, New College Building, Room 7402, Philadelphia, PA 19102, USA
e-mail: eddiechangmd@yahoo.com

Introduction

Oxidative stress associated with the administration of high levels of inspired oxygen has been linked to a variety of disease states in lung, brain, heart, and eyes of infants [1–4]. While this association has been noted, the specific mechanisms of tissue damage have not been fully elucidated.

For both human adults and infants, supplemental inspired oxygen has routinely been used in the clinical setting to prevent hypoxemia and tissue hypoxia [4, 5]. Newborn infants potentially are exposed to high levels of oxygen for varying durations during medical or surgical management. However, hyperoxia has long been associated with physiological changes in patients such as an initial decrease in minute ventilation followed by a secondary hyperventilation (hyperoxic hyperventilation) [6, 7], a decrease in arterial blood pCO_2 [8, 9], a decrease in cerebral blood flow [10, 11], reduction in cardiac output, and compromised ventricular work rates [4].

Hyperoxia may be implicated as a potential contributor to free radical-mediated brain damage in premature newborn infants. Using microelectrodes selective for reactive nitric oxide and oxygen directly implanted in the cerebral cortex of rats, $^{\bullet}NO$ and O_2 concentrations were significantly elevated in response to hyperoxia, even at ambient pressure [12]. Additionally, oxidative and nitrative injury to developing oligodendrocytes has been found to play a major role

in periventricular leukomalacia [13]. In vitro, there seems to be particular sensitivity of the preoligodendrocytes of the premature brain to the toxic effects of exogenous reactive oxygen species or glutathione depletion [14].

Increasing partial pressure of O_2, in itself, is not sufficient to cause direct chemical oxidation of biological molecules. Hyperoxia-induced cellular damage is likely due to increased partial reduction of O_2 to superoxide radical $^{\bullet}O_2$ in metabolically dependent reactions. The source of reactive oxygen species during hyperoxia is most likely the mitochondria, with ubisemiquinone being a probable source of electron leak from the mitochondrial respiratory chain [15, 16]. In mitochondria, superoxide escapes the respiratory chain and is converted into hydrogen peroxide, which subsequently may combine with transitional metals and form highly reactive oxidants. In studies by Li et al., HeLa cells engineered with impaired mitochondrial respiration were significantly resistant to free radical production and subsequent cellular damage when exposed to increased oxygen tension when compared to wild type cells [17–19].

Reactive oxygen species production inherent to oxidative stress is associated with neuronal programmed cell death. ROS may oxidize cellular components such as proteins, lipids, and DNA structurally and functionally altering them [20, 21]. Mitochondrial membrane dysfunction associated with a loss of calcium homeostasis and enhanced cellular oxidative stress have long been recognized to play a major role in cell damage associated with excitotoxicity, a process resulting from increased excitation of glutamate receptors. This mechanism of pathogenesis has been implicated in many neurodegenerative diseases such as Alzheimer's disease and Parkinson's disease [22, 23].

In the human newborn, clinical studies have recently suggested that there are self-limited but significant physiological changes such as prolonged period of apnea and elevation of inflammatory markers in the serum and tissues of humans infants and newborn animals following periods of hyperoxia [24, 25].

Studies have also suggested an association between the administration of 100% FiO_2 during delivery room resuscitation and neuronal cell death in asphyxiated newborn piglets [26]. Neuronal membrane dysfunction seems to be exacerbated during states of hyperoxia, where brains of rats exposed to both oxidative stress from 100% FiO_2 and limited antioxidant protection undergo pro-apoptotic cell death [27]. Exposure to 1 week of hyperoxia (85% FiO_2), without preceding anoxia, in a rat model has been shown to produce significant changes of blood–brain barrier permeability as measured by permeability to Gd-DTPA (gadolinium-diethylene-triamine-pentaacetic acid) on brain MRI. Also seen in the rat model was an increase in brain high-energy phosphates using in vivo ^{31}P NMR on MR images, primarily seen as an elevation of brain ATP [28]. While these changes have been noted, the mechanism of hyperoxia-induced oxidative stress and its potential effect on neuronal apoptosis in the newborn has not been fully elucidated.

In previous studies, we have shown that free radicals generated during cerebral hypoxia in newborn piglets result in peroxidation of plasma and nuclear membranes leading to increased high-affinity Ca^{2+}-ATPase activity and nuclear Ca^{2+}-influx [29–31]. The present study tests the hypothesis that hyperoxia, similar to hypoxia, results in increased lipid peroxidation, nuclear high-affinity Ca^{2+}-ATPase activity, intranuclear Ca^{2+}-influx, and expression of proapoptotic proteins in the cerebral cortex of newborn piglets.

Experimental procedure

Animal protocol

Studies were performed in 3–5 days old newborn piglets using an experimental protocol, approved by the Institutional Animal Care and Use Committee of Drexel University. Eleven anesthetized, ventilated piglets were assigned to two groups: six animals in the normoxic group and five in the hyperoxic group. Anesthesia was induced with isoflurane 4% and then lowered to 1%, while allowing the animals to breathe spontaneously through a mask. Lidocaine 1% was used for all instrumentation. A tracheostomy was performed and endotracheal tube secured. Femoral arterial polyvinyl chloride catheters were inserted for continuous monitoring and intravenous catheters used for drug administration. After instrumentation, isoflurane was discontinued and intravenous fentanyl (10 μg/kg), pentobarbital (10 mg/kg), and pancuronium (0.1 mg/kg) were administered while the animals were mechanically ventilated. In both groups, pH was maintained between 7.35 and 7.45, and PCO_2 between 35 and 45 mmHg throughout the study. After an initial stabilization period at 0.21 FiO_2, the normoxic group was continued at 0.21 for 1 h. The hyperoxic group was subjected to 1.0 FiO_2 for 1 h. At the conclusion of the 1 h period, the brain tissue was removed under anesthesia and analyzed.

Isolation of neuronal nuclei

Cerebral neuronal nuclei were isolated and purified according to the methods of Giuffrida et al. [32]. Cortical tissue was homogenized by hand in a Dounce-type glass homogenizer (200 μm clearance) in a medium containing 0.32 M sucrose, 10 mM Tris–HCl buffer (pH 6.8), and 1 mM $MgCl_2$. The homogenate was filtered through nylon bolting cloth (mesh 110) and centrifuged at 850×*g* for 60 min. The resulting pellet was resuspended in the homogenizing buffer. The suspension was mixed with a medium containing 2.4 M sucrose, 10 mM Tris–HCl buffer (pH 6.8), and 1 mM $MgCl_2$ to achieve a final concentration of 2.1 M sucrose at which neuronal nuclei are settled. The nuclei were then purified by centrifugation at 53,000×*g* for 60 min. All procedures were carried out at 4°C. The nuclear pellet was suspended in the medium, and the purity of neuronal nuclei was assessed by an Olympus phase contrast microscope. Neuronal nuclei were characterized by the presence of a centrally located nucleolus (one nucleolus per nucleus) compared to the presence of multiple nucleoli in the astrocytic and oligodendrocytic nuclei. The final nuclear preparation was 90% pure for neuronal nuclei.

Determination of high energy phosphates

Brain tissue concentrations of ATP and phosphocreatine (PCr) were determined by a coupled enzyme reaction using the method of Lamprecht et al. [33]. Frozen brain tissue was ground in perchloric acid and centrifuged at 12,000×*g* for 10 min at 4°C. The ATP concentration was calculated from the increase in absorbance at 340 nm for the 20-min period following the addition of hexokinase. Twenty micreliter of creatine kinase (CK) were added, and readings were taken at 5-min intervals until a steady state was reached. PCr concentration was calculated from the increase in absorbance at 340 nm between 0 and 20 min after the addition of creatine kinase.

Determination of lipid peroxidation products

Membrane lipids were extracted from the nuclear fraction with chloroform/methanol (2:1) using a modification of the method of Folch et al. [34]. Samples were dissolved in *n*-heptane to provide 1.0 mg lipid/ml heptane solution. Conjugated dienes were determined spectrophotometrically at 230 nm. Fluorescent compounds were determined spectrofluorometrically using an excitation wavelength of 360 nm and an emission wavelength of 435 nm. The sample intensity was compared to a quinine sulfate standard.

Determination of nuclear high-affinity Ca^{2+}-ATPase activity

Activity of Ca^{2+}-,Mg^{2+}-dependent high-affinity Ca^{2+}-ATPase in nuclear membranes was determined using a modification of the methods of Gandhi and Ross [35]. The activity of high-affinity Ca^{2+}-ATPase was determined in a 1-ml reaction medium containing 20 mM HEPES (pH 7.0), 100 mM KCl, 95 μM $CaCl_2$, 250 μM $MgCl_2$, 0 or 100 μM EGTA, 1 mM ouabain, 1 mM ATP, and 150 μg nuclear membrane protein prepared as in the tissue preparation section. The reaction was carried out at 37°C for 30 min, a period during which the rate of the reaction was linear. The reaction was stopped by the addition of 0.5 ml of 12.5% trichloroacetic acid. The samples were centrifuged, and the supernatant was analyzed for inorganic phosphate. Enzyme activity was expressed as nmoles Pi/mg protein/h. The activity of the enzyme in the presence of Ca^{2+} and Mg^{2+} is referred to as total high-affinity Ca^{2+}-ATPase activity. Nonspecific activity was determined in the absence of Ca^{2+} and Mg^{2+} and subtracted to provide specific Ca^{2+}-Mg^{2+}-dependent total high-affinity Ca^{2+}-ATPase activity.

Determination of nuclear Ca^{2+}-influx

ATP-dependent $^{45}Ca^{2+}$-influx in neuronal nuclei was determined as described by Mishra and Delivoria-Papadopoulos [36] for 120 s at 37°C in 10 mM Tris–HCl buffer (pH 7.2) containing 0.25 M sucrose, 4 mM $MgCl_2$, 100 mM KCl, 150 μg nuclear protein, 1 μM $^{45}Ca^{2+}$ with and without 1 mM ATP to determine the ATP-dependent Ca^{2+}-influx. The rate of the ATP-dependent reaction is linear for 180 s; therefore measurements were taken at 120 s. Following incubation, samples were filtered on glass fiber filters, washed, and radioactivity counted in a Rackbeta Scintillation Counter. The results were expressed as pmoles/mg protein/min.

Determination of Bax and Bcl-2 expression

Bax, and Bcl-2 protein density were determined through Western blotting techniques. Neuronal nuclear membranes were prepared as described above in the presence of protease inhibitors (1 mM phenylmethylsulfonyl fluoride, 10 g/ml aprotinin, and

0.2 mM sodium orthovanadate). Protein content was determined by the method of Lowry et al. [37], and the nuclear membrane preparation was diluted to a final concentration of 100 μg/100 μl. Five milliliters of Laemelli buffer were added to each 20 μl of nuclear membrane protein. Equal amounts of each neuronal nuclear protein (35 μl of the 100 μg/100 μl preparation) were separated by 12% SDS-PAGE and transferred electrophoretically to nitrocellulose membranes. Nitrocellulose membranes in duplicate were then blocked with 8% nonfat milk in PBS. The membranes were subsequently incubated with antibodies specific to Bax or Bcl-2 (Santa Cruz Biotechnology, Santa Cruz, CA, USA). Recombinant human Bcl-2 BV-lysate (BD PharMingen, San Diego, CA, USA) and human promyelocytic leukemia (ATCC (R) F-13737 240-CCL HL-60 018554, HL-60 promyelocytic leukemia human peripheral blood, Rockland, Gilbertsville, PA, USA) served as positive controls for Bcl-2 and Bax proteins, respectively. Immunoreactivity was detected by incubation with horseradish peroxidase-conjugated secondary antibody (Rockland). Specific complexes were detected by enhanced chemiluminescence method using the ECL detection system (Amersham Pharmacia Biotech, Little Chalfont, Buckinghamshire, UK) and analyzed by imaging densitometry (GS-700 densitometer, Bio-Rad, Hercules, CA, USA). The densitometric scanning data were expressed as autoradiographic values (OD × mm^2) per immunoblot protein representing Bax or Bcl-2 protein density.

Statistical analysis

Data were presented as mean ± standard deviation. Statistical analysis between the groups was performed by unpaired *t* tests. A *P* value of less than 0.05 was considered statistically significant.

Results

ATP and phosphocreatine

Cerebral tissue energy metabolism was documented by determining the concentrations of tissue high-energy phosphates, ATP and PCr. The ATP concentrations (μmoles/g brain) were 4.7 ± 0.4 in normoxic and 4.9 ± 0.4 in hyperoxic groups. The PCr concentrations (μmoles/g brain) were 4.1 ± 0.3 in normoxic and 4.0 ± 0.4 in hyperoxic groups. As shown in Fig. 1, ATP and PCr levels (μmoles/g brain) are compared in the experimental groups. Both the normoxic and hyperoxic groups have a comparable level of cerebral high-energy phosphates (*P* = NS).

Nuclear membrane lipid peroxidation

The level of lipid peroxidation products in neuronal nuclei of normoxic and hyperoxic animals is shown in Fig. 2. Nuclear membrane conjugated dienes (nmoles/mg protein) were higher in the hyperoxic (1.396 ± 0.491) than in the normoxic group (0 ± 0.004, $P < 0.004$). Nuclear membrane fluorescent compounds (μg quinine sulfate/g protein) were higher in the hyperoxic (24.46 ± 3.80) than in the normoxic group (19.95 ± 2.61, *P* = NS). There is a significant difference in conjugated diene production in the hyperoxic group when compared to the normoxic group, but no significant increase in the level of fluorescent compounds in the hyperoxic group when compared to the normoxic group.

High-affinity Ca^{2+}-ATPase activity

High-affinity Ca^{2+}-ATPase activity (nM inorganic Phosphate/mg protein/h) was measured in normoxic and hyperoxic groups and the data is shown in Fig. 3. There is a significant difference between high-affinity

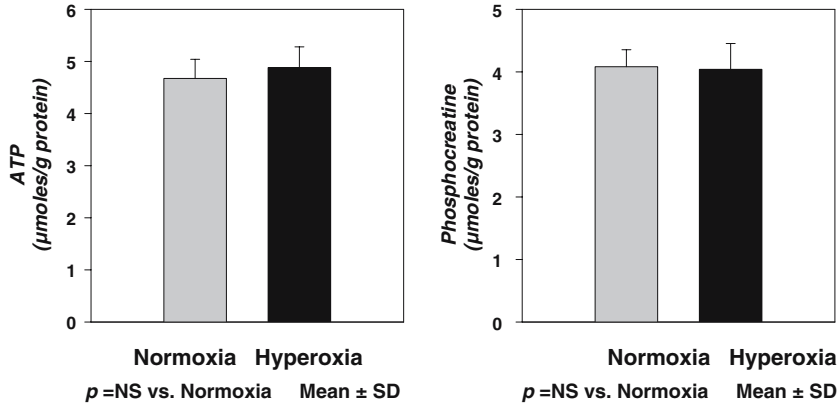

Fig. 1 High-energy phosphates levels during normoxia and hyperoxia. ATP and PCr levels are expressed in μmoles per gram brain (mean ± SD)

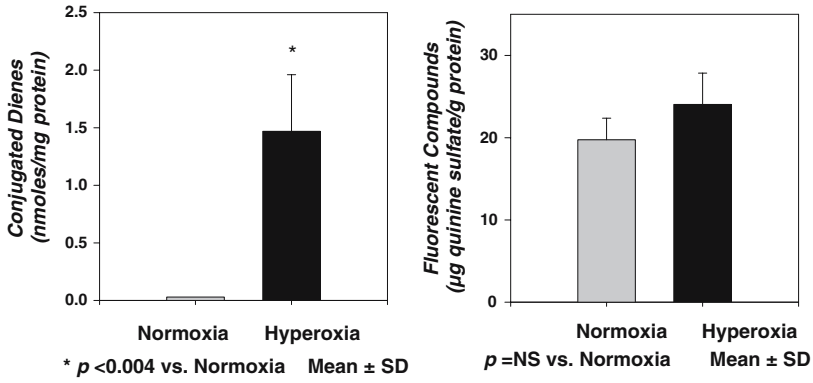

Fig. 2 The effect of hyperoxia on neuronal nuclear membrane lipid peroxidation in newborn piglets. Conjugated dienes and fluorescent compounds are measured in normoxia and hyperoxia with results reported as nmoles/mg brain (mean ± SD)

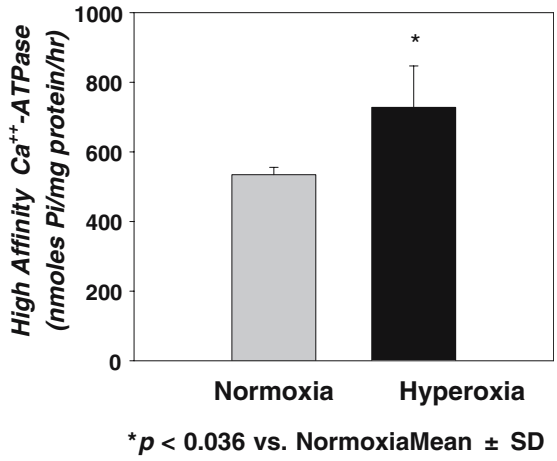

Fig. 3 Effect of hyperoxia on high-affinity Ca^{2+}-ATPase activity in neuronal nuclei of newborn piglets. High-affinity Ca^{2+}-ATPase activity is expressed in nmoles Pi/mg protein/h (mean ± SD)

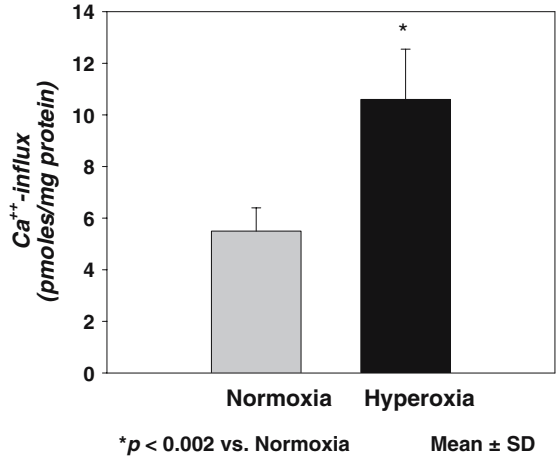

Fig. 4 Effect of hyperoxia on high-affinity Ca^{2+}-influx in neuronal nuclei of newborn piglets. High-affinity Ca^{2+}influx is expressed in pmoles/mg protein/min (mean ± SD)

Ca^{2+}-ATPase activity in the normoxic (487 ± 15) and hyperoxic (650 ± 58) groups, $P < 0.05$.

Nuclear $^{45}Ca^{2+}$-influx

Nuclear Ca^{2+}-influx is shown in Fig. 4, $^{45}Ca^{2+}$-influx expressed in pmoles/mg protein/min was 4.96 ± 0.94 in the normoxic and 11.11 ± 2.38 in the hyperoxic group, $P < 0.05$. There is a significant increase in Ca^{2+}-influx in the hyperoxic group compared to the normoxic group.

Production of Bax and Bcl-2

Representative gels showing Bax and Bcl-2 expression are shown in Fig. 5. Bax expression (OD × mm^2), shown in Fig. 6, was 244.7 ± 78.4 in hyperoxic versus 130.6 ± 16.6 in the normoxic group ($P < 0.03$). Expression of the anti-apoptotic protein Bcl-2 (OD × mm^2), shown in Fig. 7, did not change significantly in the two groups, 348.0 ± 13.8 in hyperoxia and 355.0 ± 9.2 in normoxia (P = NS). The Bax/Bcl-2 ratio increased from 0.37 to 0.7 in favor of apoptosis ($P < 0.05$).

Discussion

The results of the present study show that hyperoxia results in (1) increased lipid peroxidation, (2) increased high-affinity Ca^{2+}-ATPase activity, (3) increased Ca^{2+}-influx, and (4) increased production of proapoptotic proteins in the cortical neuronal nuclei of newborn piglets. The data indicate that hyperoxia alters neuronal nuclear membrane function leading to increased nuclear Ca^{2+} influx that is associated with an increase in expression of proapoptotic proteins. In addition, the results show that cerebral energy metabolism (measured by cerebral high energy phosphates ATP and PCr) is not different during hyperoxia in comparison to normoxia, indicating an alternative pathway of free

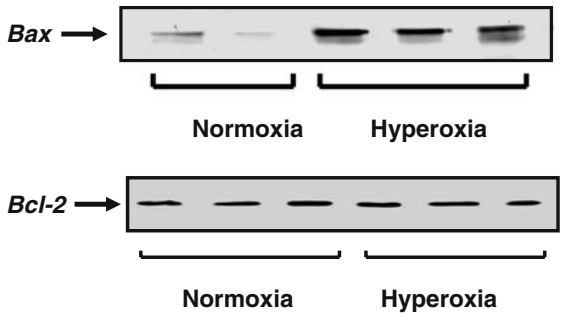

Fig. 5 Expression of Bax and Bcl-2 proteins during normoxia and hyperoxia in the cortical neuronal nuclei of newborn piglets. Proteins from neuronal nuclei from normoxic and hyperoxic animals were separated by SDS–PAGE, transferred to nitrocellulose membranes and probed with specific antibodies against Bax (*upper panel*) or Bcl-2 (*lower panel*). A representative gel for each protein analysis is shown. The *arrows* point to the bands of Bax protein (*upper panel*) and Bcl-2 protein (*lower panel*). The gel illustrates that there is less Bax protein in the normoxic than in the hyperoxic animals ($P < 0.05$). The gel illustrates that there is no difference in concentration of Bcl-2 in the three groups

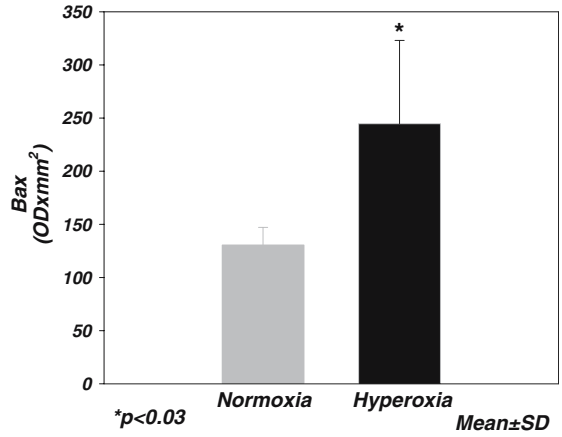

Fig. 6 Effect of hyperoxia on Bax protein expression in the cortical neuronal nuclei of newborn piglets. Bax protein expression is expressed in OD × mm^2

radical generation in hyperoxia when compared to hypoxia.

In previous studies, we have shown that hypoxia results in increased activity of high-affinity Ca^{2+}-ATPase, and increased Ca^{2+}-influx [30, 31]. We have also shown that hypoxia results in increased free radical generation and membrane lipid peroxidation in the cerebral cortex of newborn piglets [29]. In the present study we tested the hypothesis that 1 h of hyperoxia would result in increased lipid peroxidation, increased high-affinity Ca^{2+}-ATPase activity, increased Ca^{2+}-influx, and increased production of proapoptotic proteins in the neuronal nuclei of newborn piglets.

Oxidative stress associated with the administration of high concentrations of inspired oxygen affects

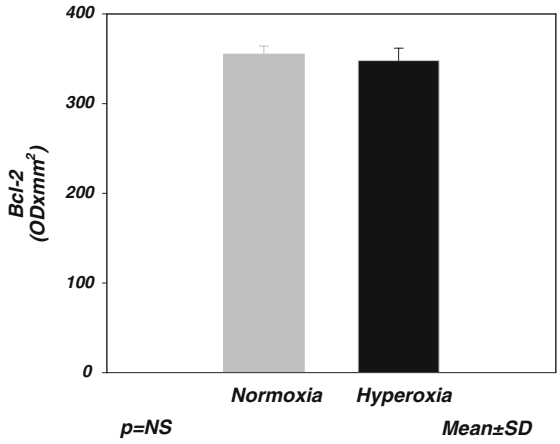

Fig. 7 Effect of hyperoxia on Bcl-2 protein expression in the cortical neuronal nuclei of newborn piglets. Bcl-2 protein expression is expressed in OD × mm^2

numerous physiological functions, which are regulated by redox-responsive signaling pathways [20, 21, 40]. Reactive oxygen species may disrupt regulation of DNA repair mechanisms, signal transduction, DNA and RNA synthesis, protein synthesis, and enzyme biosynthesis [40]. Oxidative stress damages lipids, proteins, and other cell constituents, and ultimately leads to neuronal cell death [41–43].

Cerebral tissue in newborns may be more susceptible to oxidative stress [44–46]. The determinants of susceptibility should include the lipid composition of the brain cell membrane, rate of lipid peroxidation, and presence of antioxidant defenses [47]. While reactive oxygen species are generated as part of normal cellular metabolism, large quantities of these species may overwhelm native antioxidant mechanisms, which are particularly less efficient in newborns. Newborn neuronal tissue has increased accumulation of hydrogen peroxide during times of oxidative stress, which may be due to an inadequate ability to scavenge free radicals. Decreased free radical scavengers in the newborn brain may be associated with relatively lower glutathione peroxidase activity and other antioxidative enzymes [48, 49]. Additionally, the newborn brain is rich in free iron, which readily results in the generation of the potent OH free radical via the Fenton reaction, or iron catalyzed reaction with hydrogen peroxide [50]. The hydroxyl radical is extremely reactive and is able to potentially initiate alteration of cellular membrane function via the lipid peroxidation, which can be important in causing molecular damage [12].

In previous studies, we have shown that high-affinity Ca^{2+}-ATPase activity is correlated inversely with ATP and PCr levels during hypoxia, with activity increasing as tissue high-energy phosphates decreased [30]. In the

present study, increased high-affinity Ca^{2+}-ATPase activity during hyperoxia is independent of tissue high-energy phosphates, but associated with increased lipid peroxidation indicating alternative pathways of oxygen free radial generation during hyperoxia compared to hypoxia.

We have shown in the present study that there is increased lipid peroxidation during 1 h of hyperoxia, which is sufficient to increase high-affinity Ca^{2+}-ATPase activity that may lead to nuclear Ca^{2+}-influx in the cerebral cortex of the newborn piglet. Increased nuclear Ca^{2+}-influx may result in activation of nuclear CaM kinase IV, which may phosphorylate cAMP response element binding protein (CREB). Phosphorylated CREB may alter expression of proapoptotic protein Bax, and antiapoptotic protein Bcl-2 leading to an alteration of the Bax to Bcl-2 ratio, a determinant of apoptosis. The increase of the Bax to Bcl-2 ratio may initiate mitochondrial dependent apoptotic pathway by causing the loss of outer mitochondrial membrane integrity. This may result in the release of apoptogenic proteins located in the intermembrane space of mitochondria such as cytochrome c. The released cytochrome c interacts with Apaf-1 in the cytoplasm leading to the ATP-dependent formation of the apoptosome complex. The apoptosome activates caspase-9 which, in turn, activates downstream caspases such as caspase-3. Activated caspase-3 cleaves numerous nuclear enzymes such as poly-ADP-ribose polymerase (PARP) and inhibitor of caspase-activated DNAse (ICAD), leading to activation of caspase-activated DNAse (CAD) and cleavage of chromosomal DNA resulting in morphologic apoptosis. While the effects of hyperoxia and subsequent oxidative stress on the newborn brain are complex, we propose one potential mechanism of neuronal programmed cell death.

It is quite interesting to note that both cerebral hypoxia and hyperoxia result in increased nuclear membrane lipid peroxidation, increased nuclear Ca^{2+}-influx, and increased expression of proapoptotic protein Bax. Furthermore, while cerebral tissue ATP and PCr decreased during hypoxia, high energy phosphates remain unchanged during hyperoxia. We propose that the mechanism of oxygen free radical generation during hypoxia is due to NMDA receptor-ion channel mediated Ca^{2+} that: (1) activates phospholipases and generates free radicals from lipooxygenase and cyclooxygenase pathways, (2) converts xanthine dehydrogenase to xanthine oxidase leading to free radical generation, and (3) triggers nitric oxide synthase leading to free radical generation. In addition, during hypoxia free radicals can be generated in mitochondria from increased reduction of electron transport chain components such as ubiquinone. However, during hyperoxia, the predominant mechanism of oxygen free radical generation will be due to partial reduction of O_2 molecules at the end of electron transport chain at the cytochrome a/a_3 site. Thus, free radicals generated by separate mechanisms during hypoxia and hyperoxia are a common mechanism of hypoxia as well as hyperoxia-induced neuronal cell death.

In summary, we conclude that hyperoxia alters neuronal nuclear membrane function and increases production of proapoptotic proteins in the newborn piglet. We propose that free radicals generated during hypoxia as well as during hyperoxia are common mediators that lead to peroxidation of the nuclear membrane resulting in increased high-affinity Ca^{2+}-ATPase and increased nuclear Ca^{2+}-influx leading to increased expression of proapoptotic protein Bax.

Acknowledgments The study was supported by grants from the National Institutes of Health (NIH-HD 20337 and NIH-HD 38079).

References

1. Kelly FIJ (1993) Free radical disorders of preterm infants. Br Bed Bull 49:668–678
2. Albertine KH, Plopper CG (2002) DNA oxidation or apoptosis: will the real culprit of DNA damage in hyperoxic lung injury please stand up? Am J Respir Cell Mol Biol 26: 381–383
3. Bandali KS, Belanger MP, Wittnich C (2004) Hyperoxia causes oxygen free radical-mediated membrane injury and alters myocardial function and hemodynamics in the newborn. Am J Physiol Heart Circ Physiol 287:H553–H559
4. Wittnich C, Torrance SM, Carlyle CE (2000) Effects of hyperoxia on neonatal myocardial energy status and response to global ischemia. Ann Thoracic Surg 70:2125–2131
5. Dean JB, Mulkey DK, Henderson RA III et al (2004) Hyperoxia, reactive oxygen species, and hyperventilation: oxygen sensitivity of brain stem neurons. J Appl Physiol 96: 784–791
6. Dripps RD, Comroe JH (1947) The effect of the inhalation of high and low oxygen concentration on respiration, pulse rate, ballistocardiogram, and arterial oxygen saturation (oximeter) of normal individuals. J Physiol 149:277–291
7. Becker H, Polo O, McNamara SG et al (1996) Effect of different levels of hyperoxia on breathing in healthy subjects. J Appl Physiol 81:1683–1690
8. Lambertson CJ, Stroud MW III, Gould RA et al (1953) Oxygen toxicity. Respiratory responses of normal men to inhalation of 6 and 100 percent oxygen under 3.5 atmospheres pressure. J Appl Physiol 5:487–494
9. Iscoe S, Fisher JA (2005) Hyperoxia-induced hypocapnia an underappreciated risk. Chest 128:430–433
10. Fortune JB, Bock D, Kupinski AM et al (1992) Human cerebrovascular response to oxygen and carbon dioxide as determined by internal carotid artery duplex scanning. J Trauma 32:618–627

11. Leahy FAN, Cates D, MacCallum M (1980) Effect of CO_2 and 100% O_2 on cerebral blood flow in preterm infants. J Appl Physiol 48:468–472
12. Thom SR, Bhopale V, Fisher D et al (2002) Stimulation of nitric oxide synthase in cerebral cortex due to elevated partial pressures of oxygen: an oxidative stress response. J Neurobiol 51:85–100
13. Haynes RL, Folkerth RD, Keefe RJ et al (2003) Nitrosative and oxidative injury to premyelinating oligodendrocytes in periventricular leukomalacia. J Neuropathol Exp Neurol 62: 441–450
14. Back SA, Gan X, Li Y (1998) Maturation-dependent vulnerability of oligodendrocytes to oxidative stress-induced death caused by glutathione depletion. J Neurosci 18:6241–6253
15. Li J, Gao X, Qian M et al (2004) Mitochondrial metabolism underlies hyperoxic cell damage. Free Radic Biol Med 36(11):1460–1470
16. Turrens JF, Alexandre A, Lehninger AL (1985) Ubisemiquinone is the electron donor for superoxide formation by complex III of heart mitochondria. Arch Biochem Biophys 237:408–414
17. Freeman BA, Crapo JD (1981) Hyperoxia increases oxygen radical production in rat lungs and lung mitochondria. J Biol Chem 256:10986–10992
18. Boveris A, Oshino N, Chance B (1972) The cellular production of hydrogen peroxide. Biochem J 128:617–630
19. Cross AR, Jones OTG (1991) Enzymatic mechanisms of superoxide production. Biochim Biophys Acta 1057:281–298
20. Suzuki YJ, Forman HJ, Sevanian A (1997) Oxidants as stimulators of signal transduction. Free Radical Biol Med 22:269–285
21. Basaga HS (1990) Biochemical aspects of free radicals. Biochem Cell Biol 68:989–998
22. Klein JA, Ackerman SL (2003) Oxidative stress, cell cycle, and neurodegeneration. J Clin Invest 111:735–793
23. Krantic S, Mechawar N, Reix S et al (2005) Molecular basis of programmed cell death involved in neurodegeneration. Trends Neurosci 28(12):670–676
24. Vento M, Asensi M, Sastre J et al (2001) Resuscitation with room air instead of 100% oxygen prevents oxidative stress in moderately asphyxiated term neonates. Pediatrics 107(4): 642–647
25. Kondo M, Itoh S, Isobe K et al (2000) Chemiluminescence because of the production of reactive oxygen species in the lungs of newborn piglets during resuscitation periods after asphyxiation load. Pediatr Res 47(4):524–527
26. Munkeby BH, Borke WB, Bjornland K et al (2004) Resuscitation with 100% O_2 increases cerebral injury in hypoxemic piglets. Pediatr Res 56(5):783–790
27. Tagliatatela G, Perez-Polo JR, Rassin DK (1998) Induction of apoptosis in the CNS during development by the combination of hyperoxia and inhibition of glutathione synthesis. Free Radic Biol Med 25(8):936–942
28. Noseworthy MD, Bray TM (1998) Effect of oxidative stress on brain damage detected by MRI and in vivo ^{31}P-NMR. Free Radic Biol Med 24(6):942–951
29. Numagami Y, Zubrow AB, Mishra OP et al (1997) Lipid free radical generation and brain cell membrane alteration following nitric oxide synthase inhibition during cerebral hypoxia in the newborn piglet. J Neurochem 69:1542–1547
30. Mishra OP, Delivoria-Papadopoulos M (2002) Effect of graded hypoxia on high-affinity Ca^{++}-ATPase activity in cortical neuronal nuclei of newborn piglets. Neurochem Res 26(12):1335–1341
31. Delivoria-Papadopoulos M, Akhter W, Mishra OP (2003) Hypoxia-induced Ca^{2+}-influx in cerebral cortical neuronal nuclei of newborn piglets. Neurosci Lett 342:119–123
32. Giuffreida AM, Cox D, Mathias AP (1975) RNA polymerase activity in various classes of nuclei from different regions of rat brain during postnatal development. J Neurochem 24: 749–755
33. Lamprecht W, Stein P, Heinz F et al (1974) Creatin phosphate. In: Bergmeyer HU (ed) Methods of enzymatic analysis, vol 4. Academic, New York, pp 1777–1781
34. Folch J, Lees MJ, Sloane-Stanley GH (1957) A simple method for the isolation and purification of total lipids from animal tissue. J Biol Chem 226:497–509
35. Chandrashekhar R, Gandhi DR, Ross DH (1988) Characterization of a high-affinity Mg^{2+}-independent Ca^{2+}-ATPase from rat brain synaptosomal membranes. J Neurochem 50: 248–256
36. Mishra OP, Delivoria-Papadopoulos M (2002) Nitric oxide-mediated Ca^{++}-influx in neuronal nuclei and cortical synaptosomes of normoxic and hypoxic newborn piglets. Neurosci Lett 318:93–97
37. Lowry O, Rosenbrough NJ, Farr A et al (1951) Protein measurement with the folin phenol reagent. J Biol Chem 193: 265–275
38. Akhter WA, Ashraf QM, Zanelli SA et al (2001) Effects of graded hypoxia on cerebral cortical genomic DNA fragmentation in newborn piglets. Biol Neonate 79:187–193
39. Higuchi Y, Linn S (1995) Purification of all forms of HeLa cell mitochondria DNA and assessment of damage to it caused by hydrogen peroxide treatment of mitochondria or cells. J Biol Chem 270:7950–7956
40. Droge W (2002) Free radicals in the physiological control of cell function. Physiol Rev 82:47–95
41. Ratan RR, Murphy TH, Baraban JM (1994) Oxidative stress induces apoptosis in embryonic cortical neurons. J Neurochem 62:876–379
42. Clement MV, Pervaiz S (1999) Reactive oxygen species regulate cellular response to apoptotic stimuli: a hypothesis. Free Radic Res 30:247–252
43. Saugstad OD (2005) Mechanism of tissue injury by oxygen radical: implications for neonatal disease. Biol Neonate 88: 220–236
44. Folkerth RD, Haynes RL, Borenstein NS et al (2004) Developmental lag in superoxide dismutases relative to other antioxidant enzymes in premyelinated human telencephalic white matter. J Neuropathol Exp Neurol 63(9):990–999
45. Jankov RP, Negus A, Tanswell AK (2001) Antioxidants as therapy in the newborn: some words of caution. Pediatr Res 50:681–687
46. Mishra OP, Delivoria-Papadopoulos M (1988) Anti-oxidant enzymes in fetal guinea pig brain during development and the effect of maternal hypoxia. Brain Res 470(2):173–179
47. Mishra OP, Delivoria-Papadopoulos M (1999) Cellular mechanisms of hypoxic injury in the developing brain. Brain Res Bull 48(3):233–238
48. Mishra OP, Delivoria-Papadopoulos M, Wagerle LC (1990) Anti-oxidant enzymes in the brain of newborn piglets during ischemia followed by reperfusion. Neuroscience 35(1):211–5
49. Ferriero DM (2001) Oxidant mechanisms in neonatal hypoxia-ischemia. Dev Neurosci 23:198–202
50. Jamieson D, Chance B, Cadenas E et al (1986) The relation of free radical production to hyperoxia. Ann Rev Physiol 48:703–719